

# PCCP

Accepted Manuscript



This is an *Accepted Manuscript*, which has been through the Royal Society of Chemistry peer review process and has been accepted for publication.

*Accepted Manuscripts* are published online shortly after acceptance, before technical editing, formatting and proof reading. Using this free service, authors can make their results available to the community, in citable form, before we publish the edited article. We will replace this *Accepted Manuscript* with the edited and formatted *Advance Article* as soon as it is available.

You can find more information about *Accepted Manuscripts* in the [Information for Authors](#).

Please note that technical editing may introduce minor changes to the text and/or graphics, which may alter content. The journal's standard [Terms & Conditions](#) and the [Ethical guidelines](#) still apply. In no event shall the Royal Society of Chemistry be held responsible for any errors or omissions in this *Accepted Manuscript* or any consequences arising from the use of any information it contains.

# Lipid charge regulation of non-specific biological ion channels

Vicente M. Aguilera\*, Carmina Verdiá-Báguena and Antonio Alcaraz

Dept. Physics, Lab. Molecular Biophysics. Universitat Jaume I, 12080 Castellón, Spain.

\* aguilera@uji.es

## Abstract

Ion channels are specialized proteins that enable the movement of charges through otherwise impermeable lipidic membranes. Their action is essential in living organisms facilitating electric signaling, muscle contraction or osmotic stress response among other effects. The protein and the lipid charges configure a polarized interface that yields local ionic concentrations and electric potentials that are very different from those of the bulk electrolyte. The combined effect of gradients of ionic concentration and electric potential causes the transport of ions through channels. Here we analyze charge regulation effects in different protein-lipid conformations, stressing how important is the role of electrostatic interactions in the ion channel function that traditionally has been rationalized paying attention mainly to changes in pore size. Tuning lipid charge combined with conductance and selectivity measurements is shown to be a complementary method to evidence lipid involvement in the structure of a biological ion channel.

## 1 Introduction

It was almost 25 years ago when S. McLaughlin noted that “three of the four known forces are irrelevant to most aspects of molecular and cell biology; the fourth has been ignored by most biologists until recently”.<sup>1</sup> This evident reference to electrical interactions was especially pertinent in the beginnings of modern molecular biophysics, but today there is a widespread and increasing awareness of the fundamental role of long range interactions in nanoscale science<sup>2</sup> and, particularly, in biological macromolecules and their interfaces with ionic solutions. Historically, the understanding of cell signaling and membrane electric currents has been associated to the concept of an ion conducting pore.<sup>3</sup> Since then, a large variety of transmembrane proteins and other pore-forming peptides have been described that help to communicate the cell or its organelles with their external environment, maintain the osmotic equilibrium and perform essential physiological functions for the metabolism.<sup>4</sup> They are collectively known as ion channels even though they may display a large variety of characteristics (an extensive survey can be found in the Transport Classification Database).<sup>5</sup> Here, we review how electrostatic interactions regulate the transport properties of biological channels that display multiionic transport, i.e. pores having dimensions that allow simultaneous passage of water molecules and several types of ions which may enter the pore without losing their hydration shell.<sup>6</sup> These so-called mesoscopic channels do not show a specific selectivity for a particular ionic species and in some cases are wide enough to let small metabolites like ATP or

antibiotic molecules go in.<sup>7, 8</sup> Thus, this perspective is focused more on toxins and large bacterial porins and peptide channels rather than on the canonical mammalian and bacterial channels that perform specialized signalling functions often controlling the passage of a particular ionic species across the membrane. There are many viral protein channels as well as antimicrobial peptides that fall into this category of non-specific channels where the ideas put forward here may be of interest.

Understanding the role of lipid environment in the channel activity of proteins and peptides is essential in the determination of protein structure and function and it is a novel theme in ion channel biology.<sup>9</sup> Lipids can modify the ion channel properties by changing the local distribution of charge, the dielectric constant and other physicochemical properties of the membrane, such as its fluidity, curvature strain, etc.<sup>10-12</sup> And interestingly, this protein-lipid interaction is reciprocal, i.e., there are many perturbations of membrane lipids induced by integral membrane proteins.<sup>13</sup> This *perspective* deals almost exclusively on the electrostatic effects of lipid charge on the channel properties. The membrane electrostatic environment may influence the first stage of a peptide channel formation, the membrane binding and subsequent insertion,<sup>14,15</sup> as well as its transport and selectivity properties. Electrophysiology methods have proved to be the fundamental source of information to identify and characterize non-specific charge effects associated to the protein ionizable residues and to the lipid polar heads of biological membranes.<sup>16</sup> This technique, historically associated to the detection of neural activity of excitable tissues, has become indispensable in the study of channel transport at the molecular level.<sup>4</sup> By reconstituting the protein channel in model membranes (e.g. planar phospholipid bilayers) whose lipid composition can be controlled and modified at will, the response of a single channel to an external applied voltage difference, a salt concentration gradient or other non-equilibrium perturbations, can be monitored in real time and subsequently analyzed.<sup>17</sup> Very often merging the outcome of several experiments performed under different conditions helps to understand the ion-protein interactions.<sup>6,18,19</sup> Many experimental findings associated to lipid charge effects have been traditionally rationalized by means of mean-field electrostatic theories like Gouy-Chapman (GC) double layer theory and Poisson-Boltzmann's equation,<sup>20-22</sup> or the Poisson-Nernst-Planck flux equations.<sup>23</sup> With the advent of powerful computing techniques and the increasing number of protein ion channels whose tertiary structure has been determined at atomic resolution,<sup>24</sup> unprecedented microscopic insights have been reported about the role of electrostatic interactions in ion channel function.<sup>25,26</sup> In spite of this, there are many ion channels where the predictive capability of simulations is still insufficient and lower resolution approaches like the abovementioned continuum theories are an indispensable complement to figure out charge related effects.<sup>6,26</sup>

## 2 The classical view of conductance regulation by lipid charge

The functional properties of ion channels reconstituted in model phospholipid membranes depend on a number of characteristics of the membrane: lipid composition (polar head and acyl chain), hydrophobic thickness, intrinsic membrane curvature, hydrophobic mismatch, lateral pressure, surface charge, etc.<sup>27,28</sup> Each one of these features could be of critical or secondary importance depending on the particular aspect of the ion channel under study, e.g., ion conduction, gating, ligand binding, life-time or formation on-rate, among others. Despite this, the surface charge becomes the key factor in the vast majority of membrane proteins given that ion channel activity

basically involves translocation of charged solutes. A significant fraction of the phospholipids in many biological membranes bear a net negative charge. These surface charges are located in the polar head groups of lipids and give rise to an electrostatic potential in the aqueous phase adjacent to the membrane.

Experimental evidence of the influence of lipid charge on the conductance of ion channels has built up over the last decades.<sup>20,22,29-37</sup> It has been reported that ion accumulation or depletion near a charged membrane surface influences channel ion permeation. Depending on the channel selectivity, the lipid charge can either increase or decrease channel conductance. To mention just a few examples, an increase in channel conductance with surface charge has been reported in experiments with neutral alamethicin<sup>21</sup> and also with a much smaller, ideally cation selective channel, gramicidin A, when reconstituted in negatively charged bilayers.<sup>20</sup> In the Voltage Dependent Anion Channel (VDAC) from the mitochondrial outer membrane, the effect of membrane surface charge has been studied both in negatively charged lipids and positively charged lipids.<sup>22</sup> The residual channel conductance upon VDAC-tubulin interaction was measured and it was found that in diluted solutions a cationic lipid induced a decrease in conductance relative to the neutral membrane, whereas an anionic lipid induced an increase in conductance.

The modulation of ion concentration exerted by lipid charges has been qualitatively and semi-quantitatively rationalized in terms of GC theory.<sup>20-22,38,39</sup> According to GC theory, the extent of counterion accumulation or coion depletion near a charged surface (the lipid-solution interface in this case) is critically dependent on the ratio between the Debye length of the solution,  $\lambda_D$ , and the average distance from the channel mouth to the nearest charged lipid polar head. For an ideal planar membrane, with homogeneous surface charge density  $\sigma$ , in contact with a solution of ionic strength  $I$ , the electric potential  $\varphi$  at a distance  $z$  from the surface (in  $RT/F$  units) predicted by GC theory is

$$\varphi(z) = 4 \tanh^{-1} \left[ \tanh(\varphi_o / 4) \exp(-z / \lambda_D) \right] \quad (1)$$

where  $\varphi_o$  is the dimensionless electric potential at the membrane surface, given by

$$\varphi_o = 2 \sinh^{-1} \left[ \sigma / (2F\lambda_D I) \right] \quad (2)$$

and Debye length is  $\lambda_D = (\epsilon\epsilon_o RT / IF^2)^{1/2}$ . In the above expressions  $R$  is the gas constant,  $T$  is the absolute temperature,  $F$  is Faraday constant and  $\epsilon\epsilon_o$  is the electric permittivity of water. By solving numerically Poisson-Boltzmann's equation near a charged planar surface with an embedded neutral hole representing the channel mouth,<sup>21</sup> one can calculate how the electric potential changes with respect to the normal distance from the lipid surface and also with the radial distance from the edge of the charged surface towards the center of the channel mouth (Figure 2.1). This allows estimating the counterion and coion concentrations over the pore mouth from the local electric potential. By using an empiric<sup>20</sup> or a theoretical<sup>21,22</sup> relationship between channel conductance and ion concentrations at the pore mouth, the lipid charge effect on channel transport properties can be studied. Even though the use of GC theory is widely admitted, it exhibits some limitations, the most important of which are considering ions as point charges exposed just to Coulombic interactions in the diffuse layer and regarding the solvent as a structureless continuum with homogeneous dielectric permittivity. Some theoretical developments have sought to overcome these limitations, particularly

those relative to the effect of the discreteness of surface charge both in protein ion channels and in biological membranes.<sup>1</sup> However, despite the fact that charge on membranes is discrete, models that assume a uniform density of charge in the plane of the membrane predict potentials in agreement with experiments.<sup>40-42</sup> Furthermore, besides numerous experimental verifications, GC theory has been also validated by Molecular Dynamics simulations.<sup>43</sup>

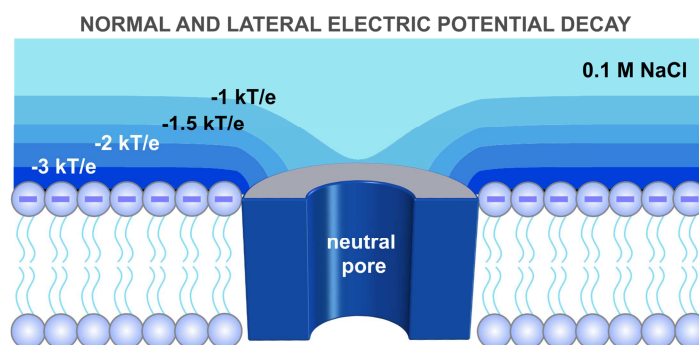


Figure 2.1

Cartoon of a wide channel embedded on a charged lipid bilayer with an isopotential contour plot of the electric potential decay in the normal direction from the lipid surface and in the lateral direction from the protein-lipid interface. Labels indicate the value of the electric potential at the limit between regions with different color. The potential was calculated for a negatively charged ( $1e/0.5 \text{ nm}^2$ ) planar surface with a neutral circular patch of radius  $1.4 \text{ nm}$  bathed by a  $0.1 \text{ M NaCl}$  solution. The contour plot size is  $6 \times 2 \text{ nm}$ . Adapted from ref. 21.

### 3 Lipid charge effects probed by conductance measurements

The classical way to investigate the interactions between the channel and the permeating ions is to analyze how channel conductance changes with salt concentration. In neutral or weakly charged pores, the channel conductance should be proportional to the solution conductivity and hence to the ion concentration.<sup>4</sup> In charged pores, one could speculate that the relationship between conductance and concentration should basically depend on the amount of carriers that are inside the channel once the electroneutrality requirements are fulfilled. Thus, some studies allegedly report a linear dependence of the channel conductance on the square root of salt concentration that could be tentatively attributed to charge screening effects. The rationale would be supposedly related to the proportionality between the inverse Debye length and the square root of ionic strength.<sup>44,45</sup> However, other experiments show no unique trend but a variety of charge screening effects depending on the pore size, the ionization state of the pore charges and the complicated balance between protein and lipid charges. In the following section we pay attention to all these effects by analyzing the conductance concentration dependence in four protein channels whose well known structure is rather different.

### 3.1 Four channels of known 3D structure

The first example brought here is the bacterial porin OmpF, a multiionic, weakly cation selective channel, well characterized both functionally and structurally,<sup>46-50</sup> which forms large pores in the outer membrane of *E. Coli*. We measured the channel conductance in ion channels reconstituted in neutral (DPhPC) and charged (DPhPS) membranes over a wide range of salt concentration (30 mM-1.5 M KCl), as shown in Figure 3.1A. In all cases, regardless the lipid composition and the salt concentration the pore displays almost ohmic conduction, so that the conductance is independent of the applied voltage even at the lowest concentration, 30 mM (see Figure 3.1B). Taking into account the size of the OmpF beta-barrel (several nanometers width), the lipid headgroup charges surrounding the channel mouths are likely to exert a minor influence on the channel conductance. Indeed, in concentrated solutions the differences between DPhPC and DPhPS are very small (within experimental error) and in both cases the conductance apparently scales with salt concentration, although the actual dependence is not linear, but somewhat like  $G \sim c^{0.7}$ . This indicates that the interaction of the permeating ions with lipid and protein charges must be described by something more elaborated than the aforementioned square root of ionic strength that correlated with the inverse of Debye length. Interestingly, the effect of the lipid charges is visible in diluted solutions. At decimolar salt concentrations the channel conductance in pores reconstituted in charged membranes increases by a factor of 2 with respect to neutral membranes.

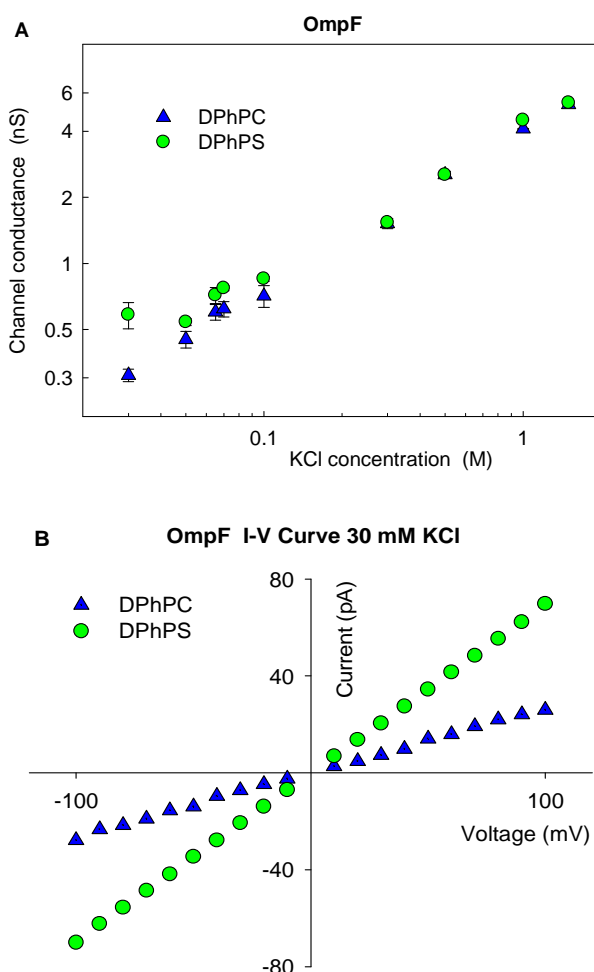


Figure 3.1

OmpF single channel conductance in neutral and charged lipid membranes. A) Double logarithmic plot of the change of the OmpF single channel conductance with the conductivity of the bathing KCl solution at neutral pH. Two sets of measurements are shown, corresponding to channel reconstitution in negatively charged DPhPS membranes (circles) and in neutral DPhPC membranes (triangles). B) Current-voltage curve obtained from single channel experiments at 30 mM KCl in DPhPC and DPhPS membranes as labeled.

A completely different channel structure is formed by the antibiotic gramicidin A (gA). This peptide dimer opens a very narrow aqueous pore that only allows for single file transport of ions. Measurements of gA conductance in neutral and charged lipids were performed by Apell et al.<sup>29</sup> for different CsCl concentrations and two decades later Rostovtseva et al.<sup>20</sup> extended the study with measurements at higher salt concentrations and a wide range of pH. Rostovtseva's results are shown in Figure 3.2. In this case the effect of the lipid is much more evident. Only at very high salt concentration the conductance in both membranes are similar, whereas for dilute solutions the effect of the lipid charge is increasing the channel conductance in one order of magnitude. Interestingly, it was found<sup>29</sup> that the addition of a small (1 mM) amount of  $\text{Ca}^{2+}$  ions to the CsCl solution rendered virtually the same gA conductance in charged and neutral lipid. This is consistent with a reduction in the negative surface potential induced by the divalent cations although it cannot be excluded a gA blocking effect by  $\text{Ca}^{2+}$  ions. The effect of the lipid is considerably higher than in OmpF because of the much smaller size of the channel. Recall that gA is a cylinder-shaped pore with radius about 0.2 nm whereas OmpF porin has an hour-glass shape of about 0.7 nm in the narrowest part of the pore with vestibules about 2 nm wide. As it could be expected, the dependence of channel conductance on salt concentration is completely different to that observed in OmpF. As figure 3.2 shows, in charged lipids the channel conductance is almost insensitive to the salt concentration. Quite the opposite, the experiments in neutral lipids show an almost linear dependence at low concentration that saturates as concentration increases and finally almost matches the results with charged lipids. Although these results qualitatively agree with GC theory, there are many more subtle issues apart from pure electrostatic salt screening that should be taken into account for a correct interpretation of lipid charge influence on gA conductance. The effect of lipid lateral tension, given the small size of this channel, and a certain lipid selectivity not directly related to the net charge of the lipid headgroups<sup>51</sup> are two examples of phenomena that fall beyond the scope of this perspective.

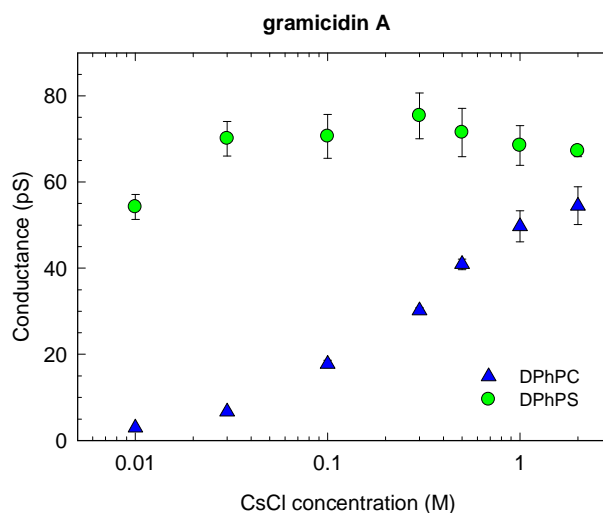


Figure 3.2

Double logarithmic plot of the change of gramicidin A channel conductance with CsCl concentration at pH 7.4. Circles denote measurements in negatively charged DPhPS membranes and triangles correspond to neutral DPhPC membranes. Adapted with permission from ref. 20.

The above examples of a bacterial porin and a small antibiotic share the feature that the channel structure is rather symmetric as regards the pore entrances. But when the channel structure is asymmetric and the lipid-protein interface differ at the two channel entrances, the effect of lipid charge on conductance may be voltage dependent and may also change with the ion current direction. This is what happens in the alpha-hemolysin channel ( $\alpha$ HL) from *Staphylococcus aureus*. Its current-voltage relationship is nonlinear, rectifying, and depends on the bulk pH and the ionic strength.<sup>52</sup> In addition to its internal asymmetric charge distribution of amino acid residues, it has a bulky cap in the membrane side where the protein is inserted and a smaller stem of cylindrical shape on the other side.<sup>53</sup> Besides, there is another difference with respect to OmpF and gA. The  $\alpha$ HL channel is anion selective. All these factors make the picture more complex than in the two previously analyzed channels, since there could exist a certain compensation between the protein and the lipid charges working in opposite directions. Even in a neutral membrane, the single conductance measurements plotted in Figure 3.3 (triangles)<sup>54</sup> show a slight (ca 20%) difference between  $\alpha$ HL conductance at +100 mV and -100 mV. When reconstituted in negatively charged lipids (DPhPS), the rectification is enhanced as shown by the circles in Figure 3.3. Because the channel distribution of charged residues is different on either pore mouths, a simple explanation in terms of anions as major current carriers and their depletion induced by the negative lipid charge is not possible.

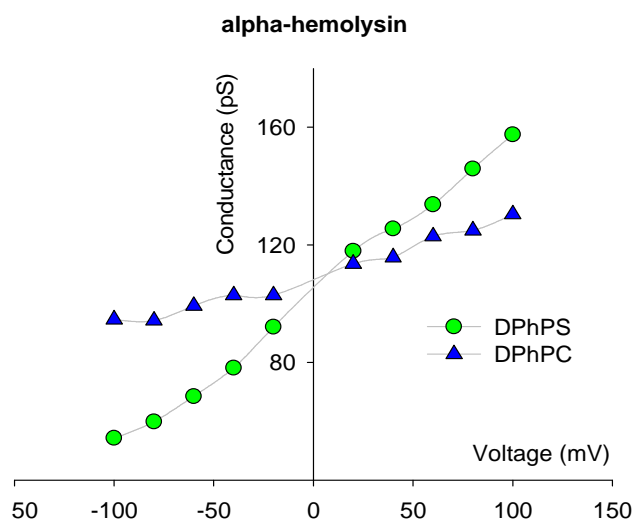


Figure 3.3

Voltage dependent single channel conductance of alpha-hemolysin in 0.1 M KCl at pH 7.5. The same symbol code as in previous figures is used: circles for DPhPS and triangles for DPhPC membranes. Adapted with permission from ref. 54.

Interestingly, lipid charge may alter channel conductance not only by inducing a change in the amount of charge carriers at the channel entrance. An increase in surface charge, and its concomitant polar head repulsion, may modify the membrane lateral stress and spontaneous curvature changing then the relative probabilities of different channel conductance states. Both kinds of effects have been reported in Alamethicin channels upon pH titration of DOPS polar heads in the membrane.<sup>55</sup> Neutralization of the lipid head group charge by proton binding reduces head-head repulsion and shifts DOPS from the lamellar structure displayed at neutral pH to a hexagonal  $H_{II}$ -phase of high curvature (confirmed by X-ray diffraction at pH 2) where higher conductance levels of the channel are much more probable. This result is consistent with the current barrel-stave model for the alamethicin channel. According to this barrel-stave structure, higher conductance states would correspond to bigger alamethicin aggregates (i.e. a larger number of assembled monomers) with a less energy cost of membrane deformation. Figure 3.4 shows single conductance measurements of the two lowest conductance states, labeled L0 and L1, in varying NaCl concentrations at pH 6.2.<sup>21</sup> Apart from a difference of up to an order of magnitude between L0 and L1 conductance, the effect of lipid charge is seen in an almost two-fold increase of channel conductance at physiological salt concentrations. It is much bigger in L0 state than in L1, which is consistent with the larger size of the pore opening in the latter case and the greater distance between the pore center and the nearest charged lipid polar head. GC theory accounts fairly well for the increase in conductance at different salt concentrations and pH. Furthermore, in this particular case it allows to estimate the increase in the number of alamethicin assembled monomers from L0 to L1 barrel stave conformations. It is worth mentioning that a neutral form of alamethicin was used in the above experiments. This detail should not be overlooked because it allows analyzing the proton binding just to the lipid head groups and not to any other ionizable residues of the protein channel. Somewhat, this is an exception

because in most experiments channel charges and lipid charges can hardly be separately manipulated by proton titration or salt screening.

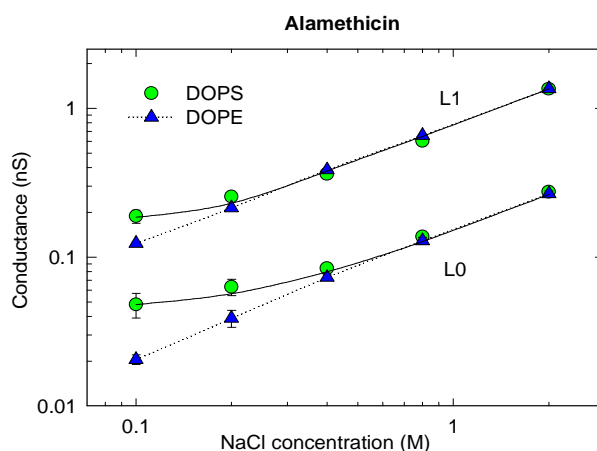


Figure 3.4

Double logarithmic plot of the change of two Alamethicin channel conductance states (L0 and L1) with NaCl concentration at pH 6.2. Circles denote measurements in negatively charged DOPS membranes and triangles correspond to neutral DOPE membranes. Adapted with permission from ref. 21.

### 3.2 Lipid charge and proteolipidic structures

The findings in these four examples of channels whose structural information is available can be summarized as follows: a) Channel conductance is different when channels are reconstituted in charged membranes and in neutral membranes; b) Low electrolyte concentrations enhance the effect of the lipid charges whereas concentrated solutions screen the lipid charges up to the point that channel currents in charged and neutral lipids become almost indistinguishable; c) As lipid charged headgroups surrounding the pore entrance are responsible for the alteration of local ion concentrations, the smaller the channel mouth the higher the effect of the charged lipid; d) The cationic or anionic channel selectivity is a key factor in the increase or decrease of ionic conductance.

This knowledge can be used to rationalize the ion channel activity of a protein in which lipid molecules assemble with protein oligomers to form a combined proteolipidic structure. This may occur in proteinaceous channels in which the lipids form the pore vestibule or just the channel mouth (see Figure 3.5A), or alternatively, in lipidic channels in which the lipid polar heads, stabilized by peptides, could be actually lining totally or partially the pore wall (see Figure 3.5B),<sup>44, 56</sup> a structure known as toroidal pore. This concept of toroidal pore was proposed as a mechanism of action of antimicrobial peptides and large toxins<sup>15</sup>. The lipid surface bends to form the inner part of a torus so that the lipid spontaneous curvature may promote or inhibit the pore formation depending on the pore size. Lipid molecules would display positive curvature in a cross-sectional plane along the pore axis (frontal view in Figure 3.5B) and negative curvature in a plane parallel to the

membrane surface. Thus, experiments with lipids of positive and negative curvature have been used to test whether a peptide forms toroidal pores in the membrane.

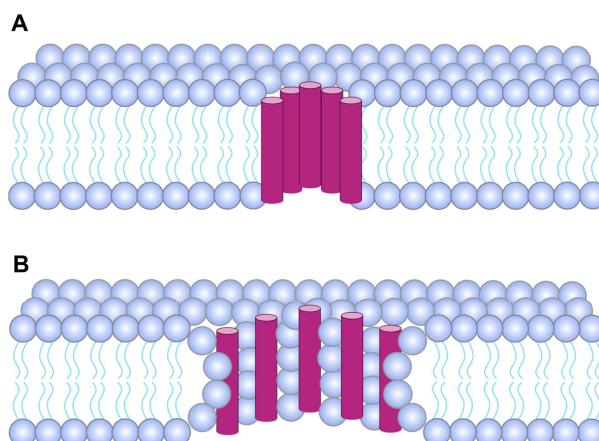


Figure 3.5

Sketch of two different kinds of proteolipidic pores where the lipid molecules and the peptide monomers are arranged following the typical barrel stave pore (A) and a toroidal pore (B).

We show here how new insights about proteolipidic pores can be gained from several series of conductance measurements of a viral protein channel, the envelope protein channel of the SARS coronavirus (SARS-CoV E).<sup>57,58</sup> It has been reported that SARS-CoV E protein oligomerizes forming a pentameric structure that alters the structure and permeability of phospholipid membranes, a remarkable function for this protein that may affect virus host interaction.<sup>57</sup> Experiments in neutral DPhPC planar bilayers show that channel conductance changes linearly with solution conductivity.<sup>58</sup> Such behavior implies that the interaction between the permeating ions and the protein is so weak that ion conduction in the pore and in bulk solution are pretty similar to each other. However, parallel experiments in charged DPhPS membranes raise some important questions because the results differ completely from the experiments reported in the previous section for OmpF, gA,  $\alpha$ HL and Alamethicin. The main unexpected result is that in experiments above physiological salt concentrations, the SARS-CoV E channel conductance is higher in neutral membranes than in charged ones (Figure 3.6). According to the classical electrostatic rationale described in the preceding section, the lipid charge induced accumulation of ions near the pore mouth should produce just the opposite effect, i.e. greater channel conductance in DPhPS. Furthermore, screening of charges at high salt concentrations does not lead to similar channel conductance in charged and neutral membranes as was the case in the other channels. Thus, in the search of alternative explanations we might ask if besides the charge-induced change in local ion concentrations at the pore entrances there are other effects that prevail and cause the observed difference in conductance. One could point to the existence of membrane-induced lipid-protein structural rearrangements. This would yield a change in the pore size that could account for variations in conductance.

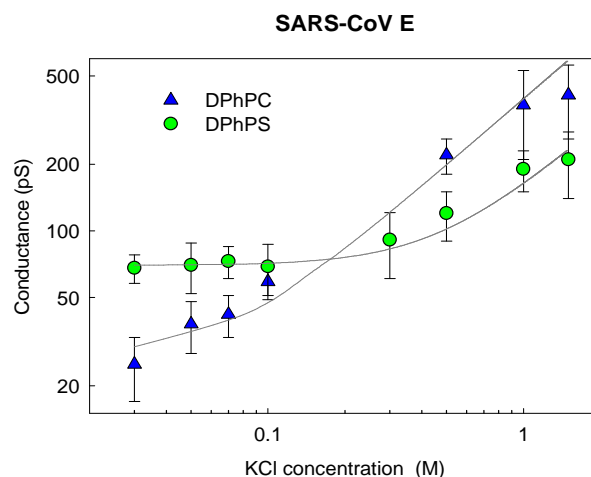


Figure 3.6

Channel conductance of SARS-CoV E protein channel in neutral DPhPC (triangles) and negatively charged DPhPS (circles) at pH 6. In DPhPS membranes and low concentration KCl solutions (30-100 mM) the channel conductance remains unaltered because the ionic concentration within the pore is controlled by the channel fixed charge. In more concentrated solutions (0.3-1.5 M), the conductance increases with the bulk KCl concentration. Adapted with permission from ref. 58.

However, this is not the unique possible scenario. It could also occur that lipid polar heads are involved in the pore structure so that lipid charges become part of the channel inner fixed charge distribution, as evidenced by the lower probability of pore formation in SARS-CoV E protein<sup>58</sup> or other viral proteins<sup>59</sup> in membranes containing DOPE, a lipid with negative intrinsic curvature. This would imply that the lipid charges directly interact with the ions that pass through the channel, modifying not only their local concentrations but also other transport properties (such as hydrodynamic hindrance of ions, lipid-protein interactions, ion-ion correlations) that most probably change ion mobilities in the pore.<sup>6</sup> Interestingly, this allows a simple explanation of the experimental results reported in Figure 3.6. SARS-CoV E protein reconstituted in DPhPS membranes becomes a negatively charged pore. Therefore, as long as the bulk concentration is small, the cation concentration inside the pore rises to match the channel fixed charge so that local electroneutrality is ensured. The increase in available carriers due to the lipid charges appears then as the reason why in this regime, channel conductance is higher in charged lipids than in neutral ones. As salt concentration increases, Donnan exclusion becomes less important and conductance increases almost linearly with the total ion concentration in the pore, similarly to a neutral pore. Remarkably, the theoretical Donnan predictions of conductance are able to reproduce the overall trend (lines depicted in the two plots of Figure 3.6).<sup>58</sup>

The change of channel conductance with concentration in SARS-CoV E protein reconstituted in DPhPS membranes raises the question of whether it is a lipid-specific effect or it is simply dependent on the lipid surface charge density. To check this lipid charge dependence, a useful strategy to study the

influence of lipid charges on channel conductance is performing experiments with membranes of varying composition of neutral and charged lipids. The advantage of this approach is two-fold. On one hand, it allows keeping the protein or peptide charge unmodified. On the other hand, it provides experimental evidence of the lipid involvement in the pore structure by looking at the way channel conductance changes with the bulk electrolyte concentration. Figure 3.7 shows measurements of single channel conductance in membranes with varying composition of (negatively charged) DPhPS and (neutral) DPhPC lipids at neutral pH. Both lipids have lamellar structure so that any effect associated to the membrane spontaneous curvature can be excluded.

Measurements were made in concentrated (1 M) and diluted (30 mM) KCl solutions for the sake of comparison. Figure 3.7A exhibits ion conductance measurements in the bacterial porin OmpF. Although the high and low salt concentration regimes are qualitatively similar, there is a significant quantitative difference: the conductance change from pure DPhPC to pure DPhPS membranes at 1 M KCl is insignificant ( $\sim 10\%$ ) when compared with the two-fold increase seen in 30 mM KCl. Because of OmpF trimeric structure is known at atomic resolution<sup>60</sup> and there are reliable estimates of the size of the trimer and of the pore mouth, these results can be rationalized in terms of the relative distance between the nearest lipid charges and the three pore openings as mentioned above. In 1 M KCl Debye length is  $\lambda_D \sim 0.3$  nm whereas in 30 mM KCl, it is  $\lambda_D \sim 1.8$  nm. At low salt concentrations the influence of the lipid negative charges may extend up to the channel mouth strongly enough to modify the electroneutrality of the bulk solution and to increase locally the concentration of cations, which are the ions preferred by this cationic channel.

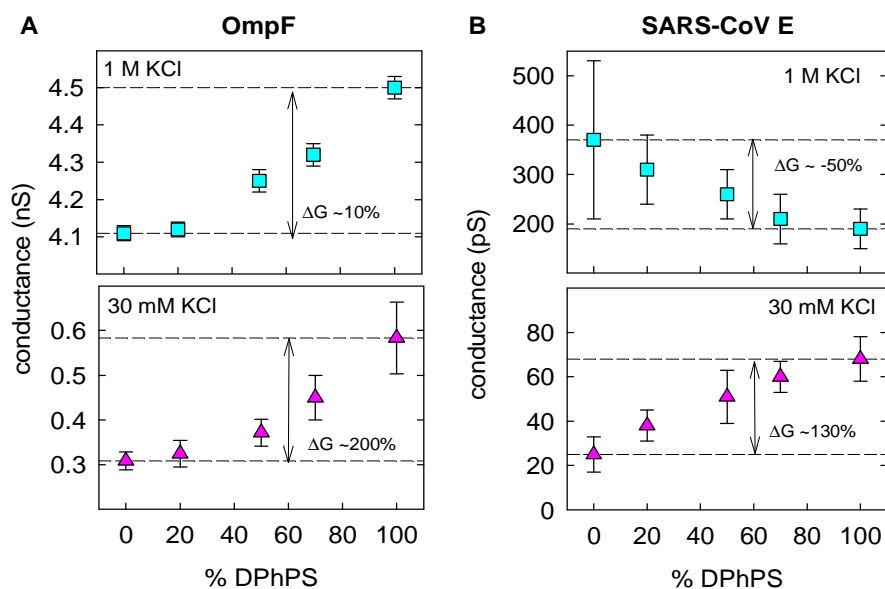


Figure 3.7

Change of single channel conductance with lipid surface charge density (proportional to the percentage of negatively charged DPhPS lipid in a DPhPC:DPhPS membrane). A) Variation of OmpF channel conductance with DPhPS percentage at low (30 mM) and high (1 M) KCl concentration. B) Variation of SARS-CoV E protein channel conductance under the same low and

high salt concentrations. All measurements were made at pH 6. Data of SARS-CoV E are taken, with permission, from ref. 58.

Figure 3.7B shows the results of SARS-CoV E protein channel conductance measurements<sup>57, 58</sup> in 1 M and 30 mM KCl solutions (top and bottom plot, respectively). A comparison between the SARS-CoV E and OmpF conductance in neutral (DPhPC) membranes reveals a difference of more than an order of magnitude between them (from 0.37 to 4.1 nS in 1 M KCl and from 25 to 300 pS in 30 mM KCl). This reflects a large difference in pore size between these two weakly selective ion channels.<sup>46,57</sup> However, the most interesting result of these four sets of measurements is that at high salt concentration, lipid charge modulates SARS-CoV E channel conductance in the opposite way it does in OmpF (as well as in gA and alamethicin): the channel conductance decreases with the amount of negatively charged lipids, which is the opposite behavior to that observed in the previous examples. Note that despite the large variability of SARS-CoV E conductance at 1 M KCl in pure DPhPC membranes, already reported and discussed elsewhere<sup>57, 58</sup>, the trend is clearly opposite to that in 30 mM KCl. Different protein-lipid conformations in DPhPC and DPhPS, with concomitant changes in pore size, can hardly be the reason behind that change in conductance because if that were the case, the ionic current should decrease or increase similarly at low and high salt concentrations. The most likely explanation of this decrease in channel conductance must be sought in the lipid polar head involvement in the channel pore structure, as mentioned above. If this is the case, the overall conductance should reflect a balance between two effects working in opposite directions. The tight lipid/ion interaction could increase the number of available carriers in the channel but could as well diminish their effective mobilities.<sup>6</sup> Actually, in diluted solutions the leading effect is the ion accumulation induced by lipid charges to preserve local electroneutrality (see Fig 3.6). But, on the contrary, as concentration increases and Donnan effects become negligible the key factor is probably the reduction in ion diffusivities that makes the charged pore less conductive than the neutral one. This reasoning does not categorically exclude the hypothetical existence of different protein-lipid conformations, but stresses how important is the understanding of charge regulation effects that otherwise could be mistakenly attributed to changes in pore size.<sup>58</sup>

Interestingly, the proteolipidic structure is shared by a large number of pore-forming peptides, antimicrobial peptides and other pore-forming toxins.<sup>61</sup> Actually, a similar decrease of channel conductance with lipid charge was found in experiments with Colicin E1 polypeptides by Sobko et al.<sup>62</sup> In two types of channels (differing in size) the conductance in 1 M KCl decreased as the membrane content in negatively charged DPhPG lipid was increased. Figure 3.8 shows the conductance dependence on the fraction of charged lipid for the smallest polypeptide (P178). The drop in conductance from pure DPhPC (~66 pS) to pure DPhPG (~6 pS) is even larger than that reported above for SARS-CoV E (Fig. 3.7B, top plot).

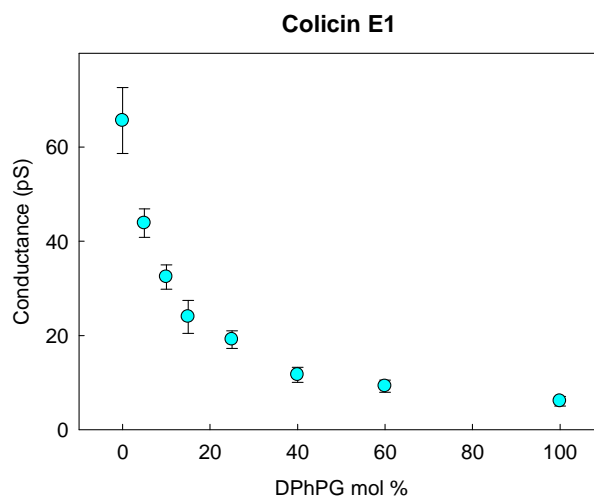


Figure 3.8

Single channel conductance of Colicin E1 channel forming domain (P178) in membranes of varying molar fraction of neutral (DPhPC) and negatively charged (DPhPG) lipids (1 M KCl, pH 4.0). Adapted, with permission from ref. 62.

Finally, we would like to focus on a completely different system, in which the mere determination of the channel conductance is a problem in itself. Pulmonary surfactant is a complex mixture of lipids and specific surfactant proteins, including the hydrophobic proteins SP-B and SP-C, in charge of stabilizing the respiratory surface of mammalian lungs. SP-C has been described to be a monomer that forms an extremely hydrophobic  $\alpha$ -helix with a transmembrane orientation. In contrast, SP-B consists of five amphipatic  $\alpha$ -helices connected by highly apolar loops and is found parallel to the surface near the interface.<sup>63</sup> Having in mind these structural details and the high hydrophobicity of both proteins, the involvement of lipid molecules in the pore structure seems to be indispensable. It was recently reported that SP-B and SP-C, both together and also individually, create a huge variety of channel-like structures in phospholipid membranes, with no characteristic size or conformation (see Figure 3.9). Indeed, both in zwitterionic and in anionic lipid membranes, a continuous distribution of conductance jumps amplitude,  $\Delta G$ , can be observed ranging from tens of pS to several nS in experiments performed in physiological salt concentrations. Although no major differences are found, the histograms reveal that, in agreement with the findings of Figure 3.7 and Figure 3.8, the most frequent values of the stepwise changes in conductance are slightly larger in neutral DOPC than in negatively charged DOPC/DOPG membranes.

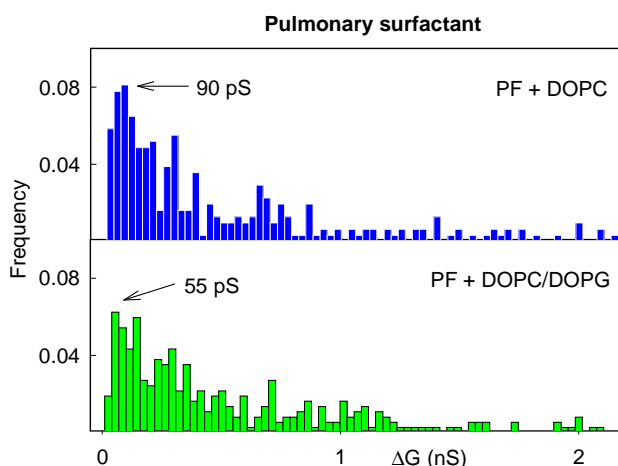


Figure 3.9

Normalized histograms representing all the conductance increments  $\Delta G$  recorded during the experiments with the hydrophobic protein fraction of native surfactant inserted in DOPC (top panel, blue) or DOPC/DOPG (bottom panel, green) bilayers for a protein/lipid ratio of 0.01% by weight in 150 mM KCl. Adapted, with permission from ref. 37.

The high variability of this system, which cannot be compared with other proteolipidic structures having better defined conductance properties, does not allow any quantitative interpretation but simply stating the fact that introducing a negatively charged lipid in the protein-lipid mixture generally reduces the conductance. However, in this particular case it is difficult to exclude other non-electrostatic effects that may an important role too.

#### 4 Channel selectivity tuned by lipid charge

The measurements shown in the preceding section show that channel conductance can be modulated by the membrane charge, particularly when lipid molecules become part of the pore structure and are not simply a passive surrounding medium hosting the transmembrane protein.<sup>57</sup> The channel selectivity, i.e. the ability to discriminate between ions of different charge, is another channel property that is strongly sensitive to the electrostatic environment the permeating ions find when crossing the membrane. Therefore, selectivity measurements in charged membranes are also a powerful tool of characterization of any transmembrane protein or peptide forming channel.

It has been noted that the ionic selectivity cannot be considered as an intrinsic property of the channel but necessarily includes both the characteristics of protein channel and of the electrolyte flowing through it.<sup>6,64</sup> However, a number of channel selectivity measurements in neutral membranes show that it is largely modulated by the density of fixed charges exposed to the permeating ions in the aqueous pore (i.e. by the amount of charged sites and their spatial distribution in the protein channel).<sup>24, 46, 52, 65, 66</sup>

The channel fixed charge density may be tuned by varying: a) the pH of the solutions (i.e. by changing the ionization state of the amino acid residues of the channel), b) the fraction of charged lipids of the

membrane, c) the salt concentration of the solutions (i.e., to screen charges more or less effectively) and d) the type of permeating ions (from monovalent or multivalent salts, etc.).<sup>46, 67</sup> Furthermore, by means of site directed mutagenesis, channels with different distribution of charged residues can be obtained.

#### 4.1 Lipid headgroups on the membrane surface

Most biological membranes contain a significant fraction of charged lipids so that the real channel selective properties are always influenced by the lipid charge no matter its magnitude. Sometimes, to isolate the channel properties, planar bilayer selectivity experiments are performed in neutral membranes. In other cases<sup>44,62,68-71</sup> experiments seek to mimic the *in vivo* environment and membranes containing a mixture of neutral and charged lipids are used.

Then, the first question that arises is to what extent lipid charge may modulate the selectivity of a wide multiionic protein channel which does not involve lipid molecules in its aqueous pore structure. To answer this question, the channel selectivity of the bacterial porin OmpF was measured in solutions of varying acidity (pH 1.5-11) in a ten-fold concentration gradient (1 M *cis*, the side of protein addition, and 0.1 M *trans*). Two series of reversal potential measurements were performed: in neutral DPhPC membranes and in negatively charged DPhPS membranes. Remarkably, almost no difference was found between both sets of measurements, as seen in Figure 4.1. Although the DPhPS negative charges probably modify the ion concentration near the channel entrance in the diluted solution (0.1 M), the repercussion in the zero current potential is negligible. Overall, the two superimposed titration curves reflect the effective pKa's of the most abundant ionizable residues of the OmpF protein: aspartates and glutamates with model pKa close to 4 and arginines with model pKa close to 12.<sup>46</sup> Therefore, it seems that when lipid headgroups are on the membrane surface and do not face the pore lumen, the channel selectivity is barely influenced by the lipid charge.

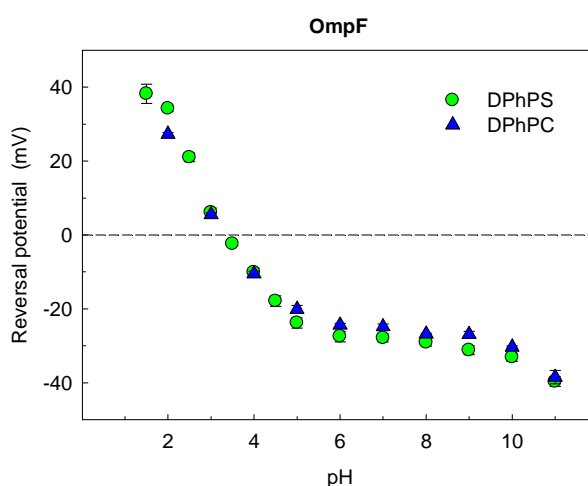


Figure 4.1

OmpF channel selectivity titration. Reversal potential was measured in neutral DPhPC membranes (triangles) and negatively charged DPhPS

membranes (circles). Under the conditions of the experiments (KCl, 1 M *cis* | 0.1 M *trans*), negative and positive reversal potential imply cationic and anionic selectivity, respectively. Each point is the average of measurements in 10-15 channels.

## 4.2 Lipid headgroups as pore building blocks

The next question concerns the effect of membrane surface charge on those channels with a proteolipidic structure like that characteristic of toroidal pores.<sup>15,72</sup> To examine the lipid charge effect on channel selectivity, reversal potential measurements were recently performed after reconstitution of SARS-CoV E channels in DPhPC and DPhPS membranes.<sup>58</sup> The experimental conditions (pH 1.5-7 and 0.5/0.05 M KCl concentration gradient) were analogous to that of Figure 4.1. Contrary to what was observed in the bacterial porin, in this case channel selectivity was strongly dependent on the net charge of the host lipid (Figure 4.2). In DPhPC membranes the channel displayed a very mild cationic selectivity at neutral pH (ratio of the permeability to positive versus negative ions,  $P_+/P_- = 1 \pm 0.1$ ) and a moderate anionic selectivity in highly acidic (pH 1.5) solutions ( $P_+/P_- = 0.3 \pm 0.1$ ). The protonation of the glutamates in the CoV E protein TM domain is likely to be the cause of this selectivity reversal. However, when the channels were reconstituted in DPhPS membranes, the ionic selectivity at neutral pH was completely different and much higher than in DPhPC: a weakly selective channel like SARS-CoV E appeared as a strongly cation selective pore. Furthermore, the change in selectivity from pH 7 to pH 1.5 was much more significant and the titration of charges even reversed the channel selectivity from cationic to anionic. The reversal potential measurements in DPhPC can be fitted according to the typical one-site titration trend seen in other channels<sup>46,73-76</sup> with an effective pKa of 4.3 (which is fairly consistent with the model pKa of glutamate). The measurements in DPhPS can be also fitted to a slightly modified version of the sigmoidal dose-response curve<sup>58</sup> with the two steep transitions being well represented by effective pKa's 4.3 and 1.7. The last value can be attributed to the shifted pKa of the carboxyl or phosphate group of DPhPS lipid polar heads. Both fitting curves are depicted by solid lines in Figure 4.2.

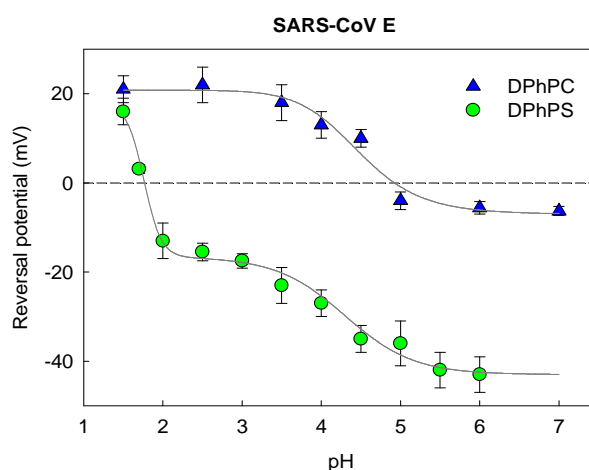


Figure 4.2

SARS-CoV E protein channel titration. Reversal potential was measured in neutral DPhPC membranes (triangles) and negatively charged DPhPS

membranes (circles). Under the conditions of the experiments (500 mM KCl *cis* | 50 mM KCl *trans*), negative and positive reversal potential imply cationic and anionic selectivity, respectively. Solid lines correspond to the best fit of the data according to the typical one-site sigmoidal titration curve (top plot) and two-site titration curve (bottom plot). Reprinted, with permission, from ref. 58.

The two series of reversal potential measurements and the values of apparent pKa from the fittings suggest that lipid molecules intercalate between the alpha helices of the SARS-CoV E TM domain in such a way that polar head groups take part in the assembling of the pore wall. This picture is in agreement with the conductance measurements in membranes of variable fraction of neutral and charged lipid. pH effects other than titration of lipid headgroups and channel ionizable residues cannot be excluded but the “titration signature” of proteolipidic pores and proteinaceous pores seems remarkably different.

The dependence of ion selectivity on pH and lipid composition in other proteins and channel-forming peptides can also be interpreted by the direct participation of lipid molecules in the channel walls, as in the case of colicin E1, the peptide eumenitin and the lipopeptide antibiotic syringomycin E. In the case of the colicin E, the selectivity is sensitive to the pH of the solution and the lipid content of the membrane<sup>76</sup> and the anionic selectivity of the colicin E is reduced in membranes containing anionic lipids.<sup>75</sup> An identical behavior is observed in syringomycin E in which the anionic selectivity of the channel is higher in neutral membranes than in membranes containing negatively charged lipids.<sup>44</sup> In the case of the peptide eumenitin, the channel exhibits cationic selectivity which is increased in membranes formed by negatively charged lipids.<sup>77</sup> In summary, selectivity experiments under variable conditions of pH and membrane lipid composition can provide valuable information about the pore structure of ion channels whose atomic structure has not been resolved yet.

#### 4.3 Correlation between conductance and selectivity

In section 3.2 we showed that pulmonary surfactant proteins SP-B and SP-C induce the permeabilization of phospholipid membranes via pore formation. An almost continuous distribution of conductance values spanning several orders of magnitude was found. In principle, the large values of conductance could correspond to multiple insertions of small pores or, alternatively, to individual wider pores. These results show that lipid composition determines the amplitude histograms, suggesting a direct incorporation of lipid into the pore structure. Selectivity measurements can be extremely useful to investigate both the pore size distribution and the role of the lipid charge in the channel function. Thus, reversal potential experiments were carried out for the entire hydrophobic surfactant protein fraction supplemented to both DOPC and DOPC/DOPG bilayers, as shown in Fig. 4.3.

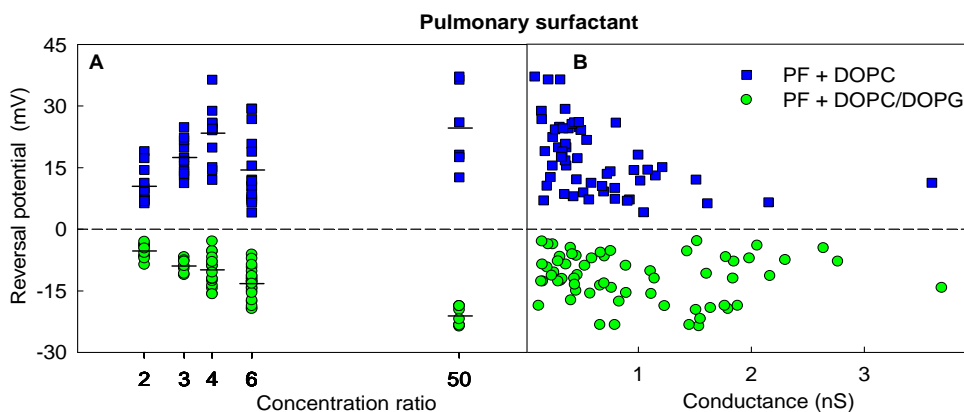


Figure 4.3

A) Reversal potential versus KCl concentration ratio (50 mM *trans* side; 100 mM-2.5 M *cis* side) for DOPC (squares) or DOPC/DOPG 85:15 (circles) bilayers supplemented with the hydrophobic protein fraction at a protein/lipid ratio of 0.01% by weight. All the measured values have been plotted, and the black line represents the average of the measurements for each concentration ratio. B) Reversal potential versus conductance for all the experiments performed with the same membranes as in panel A. Reprinted, with permission, from ref. 37.

In a neutral phospholipid bilayer like DOPC, the pores were selective to anions (upper panel of Fig. 4.3A), what is compatible with the positive net charge of both SP-B and SP-C. The addition of 15% of DOPG into DOPC bilayers resulted in an inversion of the channel selectivity: all experiments yielded negative reversal potentials, characteristic of a cation-selective channel (bottom panel of Fig. 4.3A). Similar results were obtained in DPhPC (zwitterionic) and DPhPC/DPhPS (negatively charged) bilayers<sup>37</sup>, pointing to the lipid charge as responsible for the selectivity inversion. As regards the pore size distribution, it is important to remember that the reversal potential of a population of identical channels is independent of the actual number of them and should yield the same selectivity as a single channel.<sup>4</sup> Then, the considerable dispersion found in the reversal potential values displayed in Fig. 4.3A (clearly beyond the experimental error) is consistent with the existence of multiple independent pore structures as suggested by the data of Fig. 3.9. Interestingly, the correlation between Reversal potential and conductance (Figure 4.3B) provides additional interesting clues in this sense. Although the results are visibly scattered, a general trend can be observed particularly in the case of PF+DOPC (squares in upper panel): higher values of reversal potential correspond to lower conductances (Fig. 4.3B). Narrow channels display a low conductance and a high discrimination because of the close contact between the permeating ions and the charges in the pore wall, whereas wider pores provide an easier permeation pathway at the expense of losing selectivity.<sup>37</sup>

## 5 Other specific lipid charge effects

We have focused this perspective on one aspect of the lipid charge regulation of the conductance and ion selectivity of mesoscopic biological ion channels. However, membrane permeabilization by means of ion channels involves not only coulombic interactions but also a complex interplay of other factors like mechanical and hydrophobic/hydrophilic short range interactions.<sup>78</sup> Hence, in some cases a certain degree of lipid charge specificity is found on some channel functional properties. For instance, certain anionic lipids within the family of phosphoinositides, like phosphatidylinositol 4,5-bisphosphate (PIP<sub>2</sub>) regulate a large number of ion channels by specific direct interaction with a positively charged binding site of the protein channel.<sup>9</sup> Even though the charge of the lipid is needed for the interaction (charge neutralization abolishes the channel regulation), the electrostatic nature of the lipid regulation is far from a screened coulombic one. The lipid specific interactions include those who regulate the initial stage of the channel insertion in the membrane. In addition, although it cannot be considered as lipid regulation of channel function, the binding of membrane-active proteins or peptides to anionic lipid membranes may facilitate or hinder protein insertion into the lipid bilayer. In some cases, tuning the surface potential of the membrane has proved crucial for an efficient toxin import and enhancing channel activity.<sup>14</sup>

Alternatively, there is another aspect of the lipid functional involvement in the channel: its effect on the channel opening and closing kinetics. It has been reported for the lipopeptide antibiotic syringomicin E that transitions from charged to neutral (or screened) lipids are accompanied by strong changes in the effective gating charge including inversion in the sign of potentials that open (or close) the channels.<sup>44</sup> Similarly, it has been reported also that interfacial polar interactions can affect gramicidin (gA) channel kinetics.<sup>79</sup> These experiments demonstrate that the regulation of gA lifetime involves both nonspecific (hydrophobic mismatch) and specific (headgroup-peptide) interactions. There are other effects that might be important in some cases and have been briefly mentioned here (like the charge induced lateral stress and change in curvature in alamethicin) or simply overlooked: protein conformational changes, dielectric exclusion, specific ion binding to the protein or hydrophobic interactions, to mention just some of them. The use of GC theory and Donnan equilibria may be questionable for attempting a quantitative interpretation of some of the experiments here reported but they prove to be useful to show that electrostatic effects are enough in some cases to qualitatively understand the lipid charge effect without resorting to other interactions.

## Conclusions and perspectives

Electrophysiological experiments provide new insights on the involvement of lipids in the structure and function of protein channels. The examples reviewed here of several channels with some similarities (e.g. their multiionic character, with the exception of gA) and many other differences in size, structure, oligomerization, etc., show that the effects of lipid charge on channel transport properties do not follow a simple pattern. There are key factors like the protein size, the channel selectivity and, most importantly, the kind of lipid-protein structural arrangements that should be taken into account to understand qualitatively and quantitatively the lipid charge regulation of

channel conductance. Conversely, one can take advantage of this fact to analyze lipid properties and even specific surface interactions of multivalent ions by using a channel as a probe.<sup>38</sup> Furthermore, channel conductance measurements with variable membrane lipid composition emerge as a useful tool to discriminate between proteinaceous pores and proteolipidic pores, complementary to the experimental evidence based on the use of membranes with intrinsic lipid curvature. In the case of pure proteinaceous pores, lipid charged headgroups are located only near the pore entrances, accumulating counterions as described by the Donnan equilibrium. As expected, those screening effects are more important in diluted solutions and relatively narrow pores. In proteolipidic pores, lipid charges directly interact with the ions crossing the channel, changing not only their local concentrations but also other transport properties such as ion diffusivities in the pore. In this kind of structures, we show that the experiments can be rationalized paying attention to charge regulation effects with no need to appeal necessarily to different channel conformations.

Selectivity measurements offer a similar scenario. In wide protein channels like OmpF lipid molecules do not become part of the pore structure so that the selectivity is barely influenced by the lipid charge. On the other hand, host lipid determines the ionic selectivity of proteolipidic pores. By comparing reversal potential measurements in OmpF and a viral protein channel we show how selectivity experiments can be useful to dissect the separate roles of lipid and protein charges. Correlations of conductance versus selectivity can help to discriminate between a variety of different conductance states or multiple insertions of a single unitary conductance. Overall, the electrophysiological measurements reported here for different protein-lipid conformations underlie the importance of electrostatic interactions in the ion channel functional properties. Tuning lipid charge combined with conductance and selectivity measurements is shown to be a complementary method to evidence lipid involvement in the structure of a biological ion channel. Indirectly, the influence of lipid charge on channel conductance can also be exploited to achieve rectification properties that may be used in biomimetic nanofluidic devices for sensing applications.<sup>80,81</sup>

## Acknowledgements

The authors wish to acknowledge support from the Spanish Ministry of Economy and Competitiveness (MICINN Project FIS2010-19810), Generalitat Valenciana (Prometeu 2012/069) and Fundació Caixa Castelló-Bancaixa (Project No. P1-1B2012-03).

## Notes and references

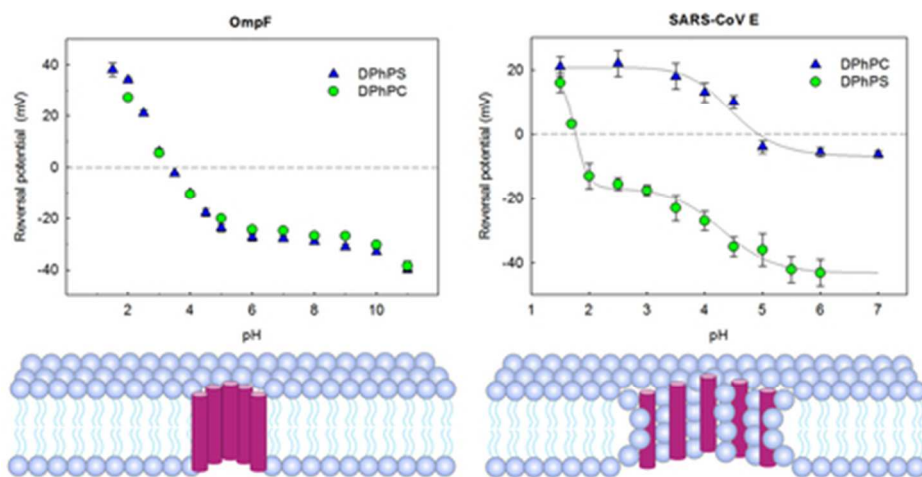
- 1 S. McLaughlin, *Annu. Rev. Biophys. Biophys. Chem.*, 1989, **18**, 113.
- 2 R.H. French, V.A. Parsegian, R. Podgornik, R.F. Rajter, A. Jagota, J. Luo, D. Asthagiri, M.K. Chaudhury, Y.-M. Chiang, S. Granick, S. Kalinin, M. Kardar, R. Kjellander, D.C. Langreth, J. Lewis, S. Lustig, D. Wesolowski, J.S. Wettlaufer, W.-Y. Ching, M. Finnis, F. Houlihan, A.O. von Lilienfeld, C.J. van Oss and T. Zemb, *Rev. Mod. Phys.*, 2010, **82**, 1887.

- 3 F. Bezanilla, *Neuron*, 2008, **60**, 456.
- 4 B. Hille, in *Ion Channels of Excitable Membranes*, ed. Sinauer Associates, Sunderland, MA, 3rd edition, 2001.
- 5 The Transporter Classification Database, <http://www.tcdb.org>.
- 6 V.M. Aguilera, M. Queralt-Martín, M. Aguilera-Arzo and A. Alcaraz, *Integrative Biology*, 2011, **3**, 159.
- 7 M. Colombini, *Mol. Cell Biochem.*, 2004, **256**, 107.
- 8 E.M. Nestorovich, C. Danelon, M. Winterhalter, S.M. Bezrukov. *Proc. Natl. Acad. Sci. U.S.A.* 2002, **99**, 9789.
- 9 S.T. Tucker and T. Baukrowitz, *J. Gen. Physiol.*, 2008, **131**, 431.
- 10 J.A. Lundbaek, *J. Gen. Physiol.*, 2008, **131**, 421.
- 11 J.A. Lundbæk, S.A. Collingwood, H.I. Ingolfsson, R. Kapoor and O.S. Andersen, *J. R. Soc. Interface*, 2010, **7**, 373.
- 12 K. Yoshimura and M. Sokabe, *J. R. Soc. Interface*, 2010, **7**, 307.
- 13 D. Marsh, *Biochim. Biophys. Acta*, 2008, **1778**, 1545.
- 14 S.D. Zakharov, T.I. Rokitskaya, V.L. Shapovalov, Y.N. Antonenko, and W.A. Cramer, *Proc. Natl. Acad. Sci. U.S.A.*, 2002, **99**, 8654.
- 15 S.D. Zakharov, E.A. Kotova, Y.N. Antonenko and W.A. Cramer, *Biochim. Biophys. Acta*, 2004, **1666**, 239.
- 16 C. Grewer, A. Gameiro, T. Mager and K. Fendler, *Annu. Rev. Biophys.* 2013, **42**, 95.
- 17 M. Montal and P. Mueller, *Proc. Natl. Acad. Sci. USA*, 1972, **69**, 3561.
- 18 P. Van Gelder, F. Dumas, M. Winterhalter. *Biophys. Chem.* 2000, **85**, 153-167.
- 19 M.L. López, E. García-Giménez, V.M. Aguilera and A. Alcaraz, *J. Phys. Condens. Mat.*, 2010, **22**, 454106.
- 20 T.K. Rostovtseva, V.M. Aguilera, I. Vodyanoy, S.M. Bezrukov, and V.A. Parsegian, *Biophys. J.*, 1998, **75**, 1783.
- 21 V.M. Aguilera and S.M. Beruzkov, *Eur. Biophys. J.*, 2001, **30**, 233.
- 22 P.A. Gurnev, M. Queralt-Martin, V.M. Aguilera, T.K. Rostovtseva and S.M. Bezrukov, *Biophys. J.*, 2012, **102**, 2070.
- 23 N. Lakshminarayanaiah, in *Equations of membrane biophysics*, ed. Academic Press, New York, 1984.

- 24 C. Maffeo, S. Bhattacharya, J. Yoo, D. Wells and A. Aksimentiev, *Chem. Rev.*, 2012, **112**, 6250.
- 25 P. Tieleman, P.C. Biggin, G.R. Smith, and M.S.P. Sansom. *Q. Rev. Biophys.* 2001, **4**, 473.
- 26 B. Roux, T. Allen, S. Bernèche, and W. Im. *Q. Rev. Biophys.* 2004, **37**, 15.
- 27 N. Tomita, M.M. Mohammad, D.J. Niedzwiecki, M. Ohta and L. Movileanu, *BBA Biomembr.*, 2013, **1828**, 1057.
- 28 A.G. Lee, *Biochim. Biophys. Acta-Rev. Biomembr.*, 2004, **1666**, 62.
- 29 H.J. Apell, E. Bamberg and P. Läuger, *Biochim Biophys. Acta*, 1979, **552**, 369.
- 30 J.E. Bell, and C. Miller, *Biophys. J.*, 1984, **45**, 279.
- 31 E. Moczydlowski, O. Alvarez, C. Vergara and R. Latorre, *J. Membr. Biol.*, 1985, **83**, 273.
- 32 R. Coronado and H. Affolter, *J. Gen. Physiol.*, 1986, **87**, 933.
- 33 W.N. Green and O.S. Andersen, *Annu. Rev. Physiol.*, 1991, **53**, 341.
- 34 S.J. Alvis, I.M. Williamson, J.M. East and A.G. Lee, *Biophys. J.*, 2003, **85**, 3828.
- 35 P.A. Gurnev, R. Ortenberg, T. Dörr, K. Lewis and S.M. Bezrukov, *FEBS Lett.*, 2012, **586**, 2529.
- 36 X.X. Yan, C.J. Porter, S.P. Hardy, D. Steer, A.I. Smith, N.S. Quinsey, V. Hughes, J.K. Cheung, A.L. Keyburn, M. Kaldhusdal, R.J. Moore, T.L. Bannam, J.C Whisstock and J.I. Rood, *MBio.*, 2013, **4**, e00019-13.
- 37 E. Parra, A. Alcaraz, A. Cruz, V.M. Aguilera and J. Pérez-Gil, *Biophys. J.*, 2013, **104**, 146.
- 38 P.A. Gurnev and S.M. Bezrukov, *Langmuir*, 2012, **28**, 15824.
- 39 A.E. Lang, J. Konukiewitz, K. Aktories and R. Benz, *Biophys. J.*, 2013, **105**, 376.
- 40 S. McLaughlin, *Curr. Top. Membrane Transport*, 1977, **9**, 71.
- 41 A.P. Winiski, A.C. McLaughlin, R. V. McDaniel, M. Eisenberg and S. McLaughlin, *Biochemistry*, 1986, **25**, 8206.
- 42 S.C. Hartsel and D.S. Cafiso, *Biochemistry*, 1986, **25**, 8214.
- 43 M. Yi, H. Nymeyer, H.X. Zhou, *Phys. Rev. Lett.*, 2008, **101**, 038103.1.
- 44 V.V. Malev, L.V. Schagina, P.A. Gurnev, J.Y. Takemoto, E.M. Nestorovich and S.M. Bezrukov, *Biophys J.*, 2002, **82**, 1985.
- 45 A. Schulte, S. Ruamchan, P. Khunkaewla and W. Suginta, *J. Membrane Biol.*, 2009, **230**, 101.
- 46 A. Alcaraz, E.M. Nestorovich, M. Aguilera-Arzo, V.M. Aguilera, and S.M. Bezrukov, *Biophys. J.*, 2004, **87**, 943.
- 47 E.M. Nestorovich, T.K. Rostovtseva, and S.M. Bezrukov, *Biophys. J.* 2003, **85**, 3718.

- 48 R. Benz, A. Schmid, and R.E.W. Hancock. *J. Bacteriol.* 1985, **162**, 722.
- 49 H. Nikaido, *Microbiol. Mol. Biol. Rev.* 2003, **67**, 593.
- 50 A.H. Delcour, *Front. Biosci.* 2003, **8**, d1055.
- 51 Z. Kóta, T. Páli and D. Marsh. *Biophys. J.* 2004, **86**, 1521.
- 52 M. Misakian and J.J. Kasianowicz, *J. Membrane Biol.*, 2003, **195**, 137.
- 53 L. Song, M.R. Hobaugh, C. Shustak, S. Cheley, H. Bayley and J.E. Gouaux, *Science*, 1996, **274**, 1859.
- 54 O.V. Krasilnikov and R.Z. Sabirov, *Gen. Physiol. Biophys.*, 1989, **8**, 213.
- 55 S.M. Bezrukov, R.P. Rand, I. Vodyanoy and V.A. Parsegian, *Faraday Discuss.*, 1998, **111**, 173.
- 56 T. Lazaridis, Y. He and L. Prieto, *Biophys. J.*, 2013, **104**, 633.
- 57 C. Verdiá-Báguena, J.L. Nieto-Torres, A. Alcaraz, M.L. DeDiego, J. Torres, V.M. Aguilera and L. Enjuanes, *Virology*, 2012, **432**, 485.
- 58 C. Verdiá-Báguena, J.L. Nieto-Torres, A. Alcaraz, M.L. DeDiego, L. Enjuanes and V.M. Aguilera, *BBA Biomembranes*, 2013, **1828**, 2026.
- 59 T. Withfield, A.J. Miles, J.C. Scheinost, J. Offer, P. Wentworth, R.A. Dwek, B.A. Wallace, P.C. Biggin, N. Zitzmann, *Mol. Membrane Biol.*, 2011, **28**, 254.
- 60 S. W. Cowan, T. Schirmer, G. Rummel, M. Steiert, R. Ghosh, R. A. Pauptit, J. N. Jansonius and J. P. Rosenbusch, *Nature*, 1992, **358**, 727.
- 61 M. Zasloff, *Nature*, 2002, **415**, 389.
- 62 A.A. Sobko, E.A. Kotova, Y.N. Antonenko, S.D. Zakharov and W.A. Cramer, *J Biol. Chem.*, 2006, **281**, 14408.
- 63 J. Pérez-Gil, *Biochim Biophys Acta* 2008, **1778**, 1676.
- 64 D. Gillespie and R.S. Eisenberg, *Eur. Biophys. J.* 2002, **31**, 454.
- 65 M. Aguilera-Arzo and V.M. Aguilera, *Eur. Phys. J. E.*, 2010, **31**, 429.
- 66 M. Vroenenraets, J. Wierenga, W. Meijberg, and H. Miedema. *Biophys. J.* 2006, **90**, 1202.
- 67 A. Alcaraz, E.M. Nestorovich, M.L. López, E. García-Giménez, S.M. Bezrukov and V.M. Aguilera, *Biophys. J.*, 2009, 96, 56.
- 68 A.A. Sobko, E.A. Kotova Y.N. Antonenko, S.D. Zakharov and W.A. Cramer, *FEBS Lett.*, 2004, **576**, 205.
- 69 A.N. Chanturiya, G. Basañez, U. Schubert, P. Henklein, J.W. Yewdell and J. Zimmerberg, *J. Virol.*, 2004, **78**, 6304.

- 70 A. Premkumar, L. Wilson, G.D. Ewart, P.W. Gage, *FEBS Lett.*, 2004, **557**, 99.
- 71 L. Wilson, C. McKinlay and P. Gage, *Virology*, 2004, **330**, 322.
- 72 R.M. Epand, *Biochim. Biophys. Acta*, 1998, **1376**, 353.
- 73 J. Cervera, A.G. Komarov, and V.M. Aguilera, *Biophys. J.*, 2008, **94**, 1194.
- 74 T.K. Rostovtseva, T.-T. Liu, M. Colombini, V.A. Parsegian and S.M. Bezrukov, *Proc. Natl. Acad. Sci. USA*, 2000, **97**, 7819.
- 75 L. Raymond, S.L. Slatin and A. Finkelstein, *J. Membrane Biol.*, 1985, **84**, 173.
- 76 J.O. Bullock, *J. Membrane Biol.*, 1992, **125**, 255.
- 77 M. Arcisio-Miranda, M. Pérez dos Santos Cabrera, K. Konno, M. Rangel, J. Procopio, *Toxicon*, 2008, **51**, 736.
- 78 N. S. Wicremasinghe, Ph.D Thesis. Rice University, 2009.
- 79 T.K. Rostovtseva, H.I. Petrache, N. Kazemi, E. Hassanzadeh and S.M. Bezrukov, *Biophys. J.*, 2008, **94**, L23.
- 80 M.X. Macrae, S. Blake, M. Mayer, and J. Yang, *J. Am. Chem. Soc.*, 2010, **132**, 1766.
- 81 M. Tagliazucchi, Y. Rabin, and I Szleifer, *ACS Nano*, 2013, **7**, 9085.



Lipid charge regulation effects in different protein-lipid conformations highlight the role of electrostatic interactions in conductance and selectivity of non-specific biological ion channels  
39x19mm (300 x 300 DPI)